JOURNAL OF INTERFERON & CYTOKINE RESEARCH
Volume 37, Number 1, 2017

DOI: 10.1089/jir.2016.0048

Systemic IL-6 Effector Response in Mediating Systemic Bone Loss Following Inhalation of Organic Dust

Adam Wells,[1,*] Debra J. Romberger,[1,2,*] Geoffrey M. Thiele,[2,3] Todd A. Wyatt,[1,2,4] Elizabeth Staab,[1] Art J. Heires,[1,2] Lynell W. Klassen,[2,3] Michael J. Duryee,[2,3] Ted R. Mikuls,[2,3] Anand Dusad,[3] William W. West,[5] Dong Wang,[6] and Jill A. Poole[1]

Airway and skeletal diseases are prominent among agriculture workers. Repetitive inhalant exposures to agriculture organic dust extract (ODE) induces bone deterioration in mice; yet the mechanisms responsible for connecting the lung-bone inflammatory axis remain unclear. We hypothesized that the interleukin (IL)-6 effector response regulates bone deterioration following inhalant ODE exposures. Using an established intranasal inhalation exposure model, wild-type (WT) and IL-6 knockout (KO) mice were treated daily with ODE or saline for 3 weeks. ODE-induced airway neutrophil influx, cytokine/chemokine release, and lung pathology were not reduced in IL-6 KO animals compared to WT mice. Utilizing micro-computed tomography, analysis of tibia showed that loss of bone mineral density, volume, and deterioration of bone micro-architecture, and mechanical strength induced by inhalant ODE exposures in WT mice were absent in IL-6 KO animals. Compared to saline treatments, bone-resorbing osteoclasts and bone marrow osteoclast precursor populations were also increased in ODE-treated WT but not IL-6 KO mice. These results show that the systemic IL-6 effector pathway mediates bone deterioration induced by repetitive inhalant ODE exposures through an effect on osteoclasts, but a positive role for IL-6 in the airway was not demonstrated. IL-6 might be an important link in explaining the lung-bone inflammatory axis.

Keywords: IL-6, mouse, organic dust, airway, lung, bone, osteoclast, precursor, inflammation, injury

Introduction

Agricultural workers, especially swine confinement workers, exhibit high prevalence of airway inflammatory diseases secondary to chronic organic dust inhalation, including chronic obstructive pulmonary disease (COPD), chronic bronchitis, and asthma (May and others 2012). This population also suffers from high rates of musculoskeletal disorders (nearly 90% of agricultural workers) and fractures (Leon and others 2011; Osborne and others 2012). An airway inflammatory-bone disease relationship has been described in human and rodent studies. Namely, in COPD and asthma, studies demonstrate that low bone mineral density (BMD) and osteoporosis can occur independently of established osteoporosis risk factors such as low body mass index, sex, age, nutritional status, and glucocorticoid use, which suggests an important association between airway inflammation and reduced bone mineralization (Lehouck and others 2011; Graat-Verboom and others 2012; Jung and others 2014). We established an animal inflammatory lung injury model whereby inhalation of complex organic dust extracts (ODE) from swine confinement facilities resulted in significant bone deterioration (Dusad and others 2013). However, the mechanisms underlying the crosstalk within the lung-bone inflammatory axis are, in general, not known. The objective of this study was to investigate a possible mechanism to explain how lung injury induced by inhalation of ODE mediates systemic bone loss.

Interleukin (IL)-6 is an important cytokine involved in impacting inflammation and immune responses, and IL-6 signals through the classical and *trans* signaling pathway to regulate downstream events (Scheller and others 2011, 2014). IL-6 has been identified as a key cytokine in chronic inflammatory lung processes, particularly in COPD. In an

[1]Pulmonary, Critical Care, Sleep & Allergy Division; [3]Rheumatology Division, Department of Medicine; [4]Department of Environmental, Agricultural, and Occupational Health; [5]Department of Pathology and Microbiology; and [6]Department of Pharmaceutical Sciences, College of Pharmacy; University of Nebraska Medical Center, The Nebraska Medical Center, Omaha, Nebraska.
[2]Veterans Affairs Nebraska-Western Iowa Health Care System, Omaha, Nebraska.
*Co-first authors.

animal model of COPD, there is elevated expression of IL-6 in lung tissue, sputum, and serum (Pauwels and others 2010). Others have proposed that systemic IL-6 release from inflamed COPD lungs is an important link between COPD and cardiac disease (Ferrari and others 2013; Lahousse and others 2013; Sin and Macnee 2013). Increased serum IL-6 has also been associated with decreased physical performance in COPD patients (Ferrari and others 2013).

IL-6 might be important in linking airway inflammation to bone disease because IL-6 is well recognized to stimulate osteoclastogenesis, and osteoclasts significantly contribute to bone resorption and bone loss (Krisher and Bar-Shavit 2014; Thiolat and others 2014). Due to its role in inflammatory-associated bone disease [eg, rheumatoid arthritis (RA)], therapeutic strategies to block systemic IL-6 have been successfully utilized to decrease bone deterioration in murine experimental models and human autoimmune arthritis (Tanaka and others 2014; Yoshida and Tanaka 2014; Briot and others 2015). Importantly, increased airway and serum IL-6 levels are found in persons and rodents exposed to agriculture organic dust environments (Wang and others 1996, 1997; Zhiping and others 1996; Poole and others 2015a).

Based upon these observations, we hypothesized that the systemic IL-6 effector response might be important in explaining the crosstalk between organic dust-induced lung disease and subsequent bone deterioration. To test this hypothesis, airway inflammatory parameters, bone deterioration consequences, and osteoclast precursor (OCP) numbers as a result of repetitive, intranasal inhalant ODE exposures were investigated in IL-6 knockout (KO) and wild-type (WT) mice. Although IL-6 KO animals were not protected from organic dust-induced lung inflammation, they were protected against ODE-induced bone deterioration and expansion of osteoclast progenitor cells. These results suggest that IL-6 might play a key role in modulating the lung-bone inflammatory axis and could represent a future target to reduce systemic bone disease following airway injury.

Materials and Methods

Organic dust extract

Aqueous ODE were prepared from settle surface dust (~1 m above the floor) from swine confinement feeding operations that housed 500–700 animals using previously described methods (Dusad and others 2013). Dust (1 g) was placed into sterile Hank's balanced salt solution (10 mL; Sigma, St. Louis, MO), incubated for 1 h at room temperature, and centrifuged for 20 min at 2,000 *g*. The final supernatant was filter-sterilized (0.22 μm) to remove coarse particles and microorganisms, and stock ODE aliquots (ie, 100% ODE) were stored at −20°C. Stock ODE was diluted in sterile phosphate-buffered saline (PBS, pH: 7.4; diluent) to a 12.5% concentration, which has previously been shown to elicit optimal lung inflammation in mice and is well tolerated (Ek and others 2004). Comprehensive characterization of this organic dust/ODE has been previously described (Poole and others 2010; Boissy and others 2014). Briefly, organic dust is comprised of particulates enriched in a wide diversity of Gram-positive and Gram-negative bacterial products. For these studies, the ODE contained ~4 mg/mL of total protein as measured by nanodrop spectrophotometry (NanoDrop Technologies, Wilmington, DE) and the mean endotoxin concentration within 12.5% ODE was 146.6 (SD 8.0) EU/mL as assayed using the limulus amebocyte lysate assay (Lonza, Allendale, NJ).

Animal model

Male WT C57BL/6 and IL-6 KO (129S6-IL-$6^{tm1Kopf}$) mice on C57BL/6 background (ages 6–8 weeks old) were purchased from The Jackson Laboratory (Bar Harbor, ME). Using an established method (Poole and others 2009), animals were intranasally treated (mice are obligate nasal breathers) once or daily for 3 weeks with 50 μL sterile saline (PBS) or 12.5% ODE. No mice exhibited respiratory distress or weight loss throughout the treatment period. All animal procedures were approved by the Institutional Animal Care and Use Committee at the University of Nebraska Medical Center, and studies were conducted in accordance to National Institutes of Health guidelines for the use of rodents. Animals were sacrificed and harvested tissues processed 5 h following final ODE treatment.

Cellular and cytokine analysis of bronchoalveolar lavage fluid

Bronchoalveolar lavage fluid (BALF) was collected by whole lung lavage with 3 × 1 mL of sterile PBS as previously described (Poole and others 2009). Total cells recovered from pooled lavages were enumerated and differential cell counts for macrophage, neutrophil, and lymphocyte populations were determined from cytospun-prepared slides (Cytopro cytocentrifuge; ELITech, Logan, UT) stained with DiffQuick (Siemens Healthcare Diagnostics, Inc., Newark, DE). To be consistent with our prior studies investigating ODE-induced airway inflammatory disease (Poole and others 2009, 2015b), tumor necrosis factor (TNF)-α, IL-6, and murine neutrophil chemoattractants [keratinocyte chemoattractant (CXCL1) and macrophage inflammatory protein-2 (CXCL2)] were quantified from cell-free BALF supernatant of the first lavage fraction by enzyme-linked immunosorbent assay (ELISA) kits (R&D Systems, Minneapolis, MN) with lower limit thresholds of 10.9, 7.8, 15.6, and 7.8 pg/mL, respectively.

Lung histopathology

After whole lung lavage, lungs were harvested, inflated with 1 mL 10% formalin, and suspended under a pressure of 20 cm H_2O for 1 day while submerged in 10% formalin for optimal preservation of lung parenchyma (Poole and others 2009). Fixed lung tissues were processed using standard techniques, embedded in paraffin, and sections (4–5 μm) were cut and stained with hematoxylin and eosin. Slides were microscopically reviewed and assessed by a pathologist blinded to the treatment assignment and scored for the degree and distribution of inflammatory changes (Poole and others 2009).

Serum

Whole blood was collected from mice at the time of euthanasia from the axillary artery. Blood (400 μL) was placed in BD Microtainer Tubes (Becton, Dickinson and Company, Franklin Lakes, NJ) and centrifuged for 2 min at 6,000 *g* and supernatant sample collected. Serum IL-6 was quantified according to manufacturer's instructions using a Quantikine ELISA kit (R&D Systems).

Micro-computed tomography

Following repetitive intranasal inhalation exposure with saline or ODE daily for 3 weeks, tibias were isolated and processed for micro-computed tomography (CT) scanning and analysis as previously described (Poole and others 2015a). The bones were scanned using high-resolution micro-CT (Skyscan 1172; Skyscan, Aartselaar, Belgium) with images acquired at a resolution of 6.07 μm (Monso and others 2003). X-ray projection images were acquired at a resolution of 6.07 μm. The X-ray source was set at 48 kV and 187 μA with a 0.5-mm-thick aluminum filter and exposed for 620 ms. Scanning was performed at 0.4° intervals, and 6 average frames were obtained for each rotation. NRECON (Sky-scan) software was used to reconstruct the scanned images. The bone position was corrected using Dataviewer (Skyscan) software to assure proper orientation along the longitudinal axis and growth plates were identified as a reference point.

Analysis on the reconstructed images using CTAn (Skyscan) software started 75 slices distal to reference point and mineralized cartilage was excluded from analysis. Final analysis was conducted on a volume of interest of trabecular bone (1.82 mm distance; 300 × 6.07 μm; 300 slides) in the metaphyseal region. An interpolated region of interest (ROI) was manually drawn to exclude the cortical shell. Three-dimensional (3D) parameters for BMD (g/cm^3), bone volume to tissue volume ratio (BV/TV, %), bone surface to bone volume ratio (BS/BV, mm^{-1}), trabecular number (TbN, mm^{-1}), trabecular separation (TbSp, mm), trabecular pattern factor (TbPf, mm^{-1}), trabecular thickness (TbTh, mm), and polar moment of inertia (MMI, mm^4) were calculated.

Details of bone measurement methods and parameter description can be found on the Skyscan Website at www.skyscan.be. Briefly, BV/TV indicates the fraction of the total volume that is occupied by mineralized bone, with lower percentages indicating deficit in mineralized bone mass. BS/BV represents the bone volume enclosed by the bone ROI surface area, with increased ratio representing bone deterioration (Dempster and others 2013). TbN is the number of trabecular plates per unit distance with decreased number representing bone deterioration (Dempster and others 2013). TbSp is the mean distance between trabeculae, with increased distance representing decreased size and number of trabeculae (Dempster and others 2013). TbTh indicates the distance across individual trabeculae giving estimation of thickness of the remaining trabeculae (Dempster and others 2013).

The TbPf detects changes in trabecular bone and describes quantitatively the ratio of intertrabecular connectivity, with an increase in TbPf suggesting increased bone deterioration (Hahn and others 1992). The polar MMI is the geometric index of bone strength to resist torsion (Bellido and others 2010).

Bone osteoclast staining

After micro-CT imaging, bones were decalcified and processed for histology. Following standard processing, embedded bones were decalcified in 15% ethylenediaminetetraacetic acid in 10% PBS buffer on a shaker at 4°C for 3 weeks, with decalcification solution being changed every 3 days (Dusad and others 2015). After decalcification, bones were sectioned (4–5 μm), and stained for tartrate-resistant acid phosphatase (TRAP) to identify bone-resorbing multinucleated osteoclasts. Osteoclasts were counted at successive fields of vision at 40 × magnification along the proximal growth plates of each representative bone. One bone per mouse ($n = 7$ mice/group) were examined with 10 fields of vision per bone section. Slides were scanned with an iScan Coreo Au slide scanner (Ventana, Tucson, AZ) and converted into digital jpeg format.

Phenotyping bone marrow cells for OCP populations

Bone marrow cells from hind limbs from WT and IL-6 KO animals repetitively treated with daily saline or ODE were flushed with 10 mL of sterile PBS and passed through a nylon mesh (70 μM; Thermo Fisher Scientific, Waltham, MA) to remove any large fragments. Red blood cells were lysed by brief suspension in cold sterile water before resuspending them in a final 1 × PBS solution. Following centrifugation, the cells were resuspended in 0.1% bovine serum albumin in PBS for staining with a LIVE/DEAD Fixable Violet Dead Cell Stain kit (Life Technologies, Carlsbad, CA), which was used to assess cell viabilities. There were no differences in cell viability between saline and ODE-treated groups or between WT and KO mice (data not shown).

Bone marrow cells from each animal were stained with monoclonal antibodies directed against T cell lineage: CD3, B cell lineage: B220/CD45R, monocyte/macrophage lineage: Mac-1/CD11b, and against markers of progenitor cells: c-fms/CD115, c-kit/CD117, and CD27 (BD Biosciences, San Jose, CA). Parallel cell preparations were treated with appropriate isotype control antibody. Compensation was performed with antibody capture beads (eBiosciences, San Diego, CA) stained separately with each individual antibody used in test samples.

The gating strategy for OCP populations utilized several published, step-wise approaches to define bone marrow OCPs (Xiao and others 2013; Jacome-Galarza and others 2014). After exclusion of debris and dead cells, gating was on triple negative (TN: CD45R$^-$, CD3$^-$, CD11b^{lo}) cell population because most of the osteoclastogenic activity of total bone marrow cells resides in this TN fraction (Xiao and others 2013; Jacome-Galarza and others 2014). CD115 (M-CSF), CD117 (c-kit), and CD27 were utilized as additional surface markers to further delineate the OCP population within the TN population. It has been demonstrated by others that most of the early osteoclastogenic activity of the TN bone marrow fraction is contained within the TN CD115$^+$CD117$^+$ population (Jacome-Galarza and others 2014). Xiao and others (2013) demonstrated that CD27 expression on TN CD115$^+$CD117$^+$ populations further discriminates cells that are highly enriched for osteoclastogenic potential. Supplementary Fig. S1 (Supplementary Data are available online at www.liebertpub.com/jir) depicts the gating strategy utilized to identify OCP populations.

Statistical methods

Data are presented as mean and standard error of mean (SEM). Statistical significance was assessed by 1-way analysis of variance (ANOVA) followed by Tukey's *post hoc* analysis when group differences were significant ($P < 0.05$), and a 2-tailed Mann–Whitney test, where

appropriate. Significance was accepted at P values <0.05. GraphPad (Version 5.02; La Jolla, CA) software was used.

Results

ODE-induced airway inflammatory cellular influx, cytokine/chemokine release, and lung pathology is not reduced in IL-6 KO mice

Mice were intranasally treated once (single treatment) or daily for 3 weeks (repetitive treatment) with saline or ODE. There was an increase in total cell counts and neutrophils in WT and IL-6 KO mice following single ODE and repetitive ODE treatment ($P<0.001$) compared to saline control treatment groups (Fig. 1A). Macrophages were significantly increased with repetitive ODE exposure ($P<0.05$ for WT, $P<0.01$ for IL-6 KO). However, there was no significant difference in the influx of total cells, neutrophils, or macrophages between ODE-treated WT and IL-6 KO animals (Fig. 1A).

ODE-induced TNF-α, IL-6, CXCL1, and CXCL2 release were increased following acute ODE exposure in WT mice, but the response was significantly attenuated following repetitive, daily ODE exposure for 3 weeks (Fig. 1B), which is consistent with previous work describing the chronic airway inflammatory adaptation response (Poole and others 2009). There was also increased TNF-α, CXCL1, and CXCL2 release in IL-6 KO mice treated once with ODE, and these levels were generally greater than the levels detected in ODE-treated WT mice with statistical significance met for the neutrophil chemoattractants, CXCL1 ($P<0.01$) and CXCL2 ($P<0.05$). IL-6 was not detected in the lavage fluid of IL-6 KO animals.

It has been well established that repetitive ODE treatment induces murine lung histopathologic changes marked by the development of lymphoid aggregates and significant increases in bronchiolar and alveolar compartment inflammation (Poole and others 2009). Here, we found that repetitive ODE exposures induced increased lung parenchymal cellular aggregates and peribronchiolar cellular infiltrates on histopathology, but this finding was not reduced in IL-6 KO mice (Fig. 2). There was no difference in lung inflammatory scores between ODE-treated WT and IL-6 KO animals (data not shown).

Serum IL-6 levels in ODE-treated animals

Previously, we reported that serum IL-6 levels are increased following a single, 1-time exposure to ODE in WT mice (Poole and others 2015a). In this study, there was a trend toward increased serum IL-6 levels in WT animals following daily, repetitive inhalant ODE exposure for 3 weeks. However, values extrapolated by ELISA reader were at or below the range level of assay detection (<7.8 pg/mL). The mean ± SEM of serum IL-6 level in saline treated WT mice were 1.33 ± 0.65 pg/mL versus 6.75 ± 1.60 pg/mL in ODE treated mice ($n=4$ mice/group). This finding of decreased serum IL-6 levels with repetitive exposures would be consistent with the described adaptation response over

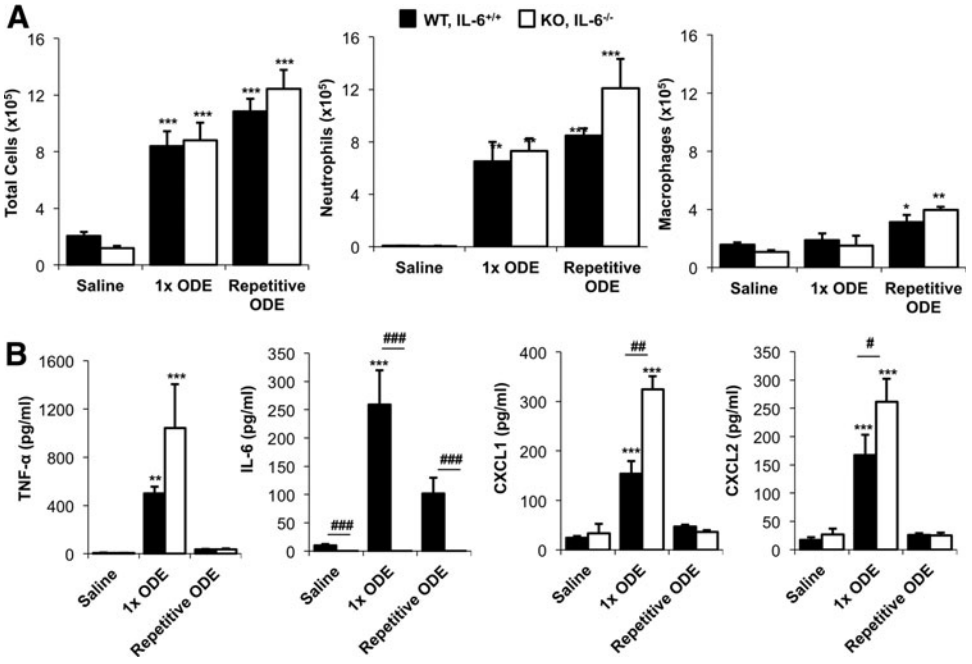

FIG. 1. ODE-induced airway cellular influx and cytokine/chemokine release is not reduced in IL-6 KO animals. WT and IL-6 KO mice were treated with intranasal inhalation of saline, ODE once (1×ODE) or ODE daily for 3 weeks (repetitive ODE) whereupon BALF was collected. **(A)** Total cell, neutrophil, and macrophage influx is shown. **(B)** TNF-α, IL-6, CXCL1, and CXCL2 levels in cell-free BALF are shown. Bar graphs are means with SEM bars. $n=8$–10 mice/group from a 2 independent experiments. Note that IL-6 KO mice are not protected against ODE-induced airway inflammatory measures. Statistical significance denoted as $^{*}P<0.05$, $^{**}P<0.01$, $^{***}P<0.001$ versus respective saline, and $^{\#}P<0.05$, $^{\#\#}P<0.01$, $^{\#\#\#}P<0.001$ is WT versus KO; all other comparisons were not statistically significant. BALF, bronchoalveolar lavage fluid; IL, interleukin; KO, knockout; SEM, standard error of mean; TN, triple negative; TNF, tumor necrosis factor.

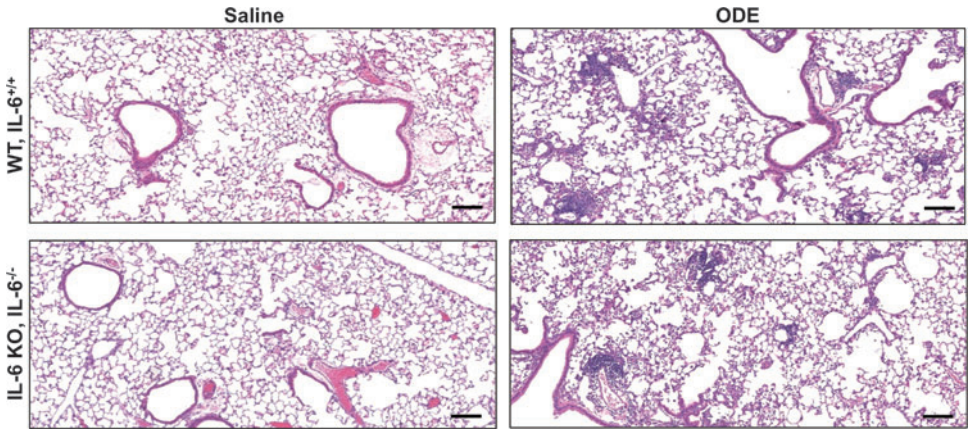

FIG. 2. Lung inflammation is not reduced in IL-6 KO mice following repetitive ODE exposures. WT and IL-6 KO animals were treated with intranasal inhalation of saline or ODE daily for 3 weeks. A representative (4–5 μm thick) H&E stained lung section of 1 mouse per treatment group is shown (10× magnification). There is no difference in ODE-induced lung parenchymal cellular aggregates and peribronchiolar cellular infiltrates between WT and IL-6 KO mice. Scale bar represents 100 μm. ODE, organic dust extract; WT, wild-type.

time to repetitive ODE exposures (Poole and others 2009). Serum IL-6 levels were not detectable in IL-6 KO animals.

Inhalant ODE exposure-induced bone quality and quantity loss is dependent on the IL-6 pathway

Despite the lack of a reduction in ODE-induced airway inflammatory consequences in the IL-6 KO mice, we next sought to assess the role of the systemic IL-6 effector response on bone parameters by micro-CT following repetitive inhalant ODE exposure. Experimental results demonstrated that IL-6 KO mice were protected from the adverse bone effects induced by inhalant ODE treatment (Figs. 3 and 4). Figure 3 shows a representative 3D reconstructed image of the ROI of the tibia from each treatment group. Utilizing this ROI, specific bone parameters were quantified (Fig. 4). There was significant loss in the bone density (BMD; $P<0.01$) and volume (BV/TV; $P<0.05$) in inhalant ODE-treated WT mice compared to saline-treated WT animals (Fig. 4A), which is consistent with previous studies (Dusad and others 2013). Representing increased bone deterioration, here was also an increase in the BS/BV ratio following ODE treatment in WT animals ($P<0.05$). Moreover, there was loss of TbN ($P<0.05$) and TbTh ($P<0.05$) in WT mice treated with ODE compared to saline-treated animals. The distance between trabeculae (TbSp; $P<0.05$) increased with ODE exposure and there was also an increase in the TbPf ($P<0.05$), which detects adverse changes in trabecular bone quality, in the WT animals. There was significant decrease in the geometric index of bone strength to resist torsion (MMI; $P<0.01$) in ODE-treated WT animals compared to saline. In contrast, repetitive inhalant ODE treatment daily for 3 weeks did not induce bone deterioration in IL-6 KO mice (Fig. 4B).

Systemic IL-6 influences inhalant ODE exposure-induced osteoclasts

To determine whether bone-resorbing osteoclasts were influenced by repetitive inhalant ODE treatment, bone sections were stained for TRAP and osteoclasts were quantified (Fig. 5A, B). Inhalant ODE-treatment resulted in increased osteoclasts in WT mice compared to saline, which was not demonstrated in IL-6 KO animals (Fig. 5B).

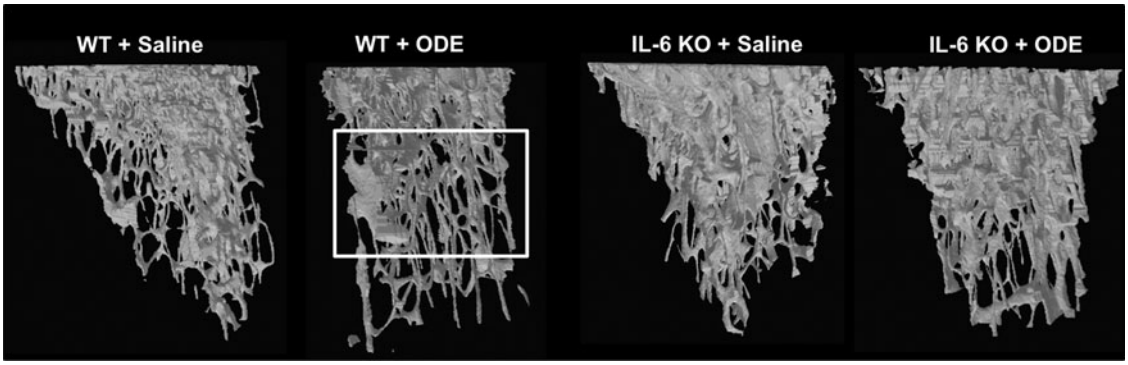

FIG. 3. Three dimensional reconstructed images of tibia of WT and IL-6 KO mice repetitively treated with inhalant ODE or saline. A representative 3D reconstructed image from region of interest of proximal tibia from 1 mouse per treatment group (minimum of 8 mice/group from 3 independent experiments). Note the substantial loss of trabecular bone in the tibia of ODE treated WT mice (*open white box*). 3D, three dimensional.

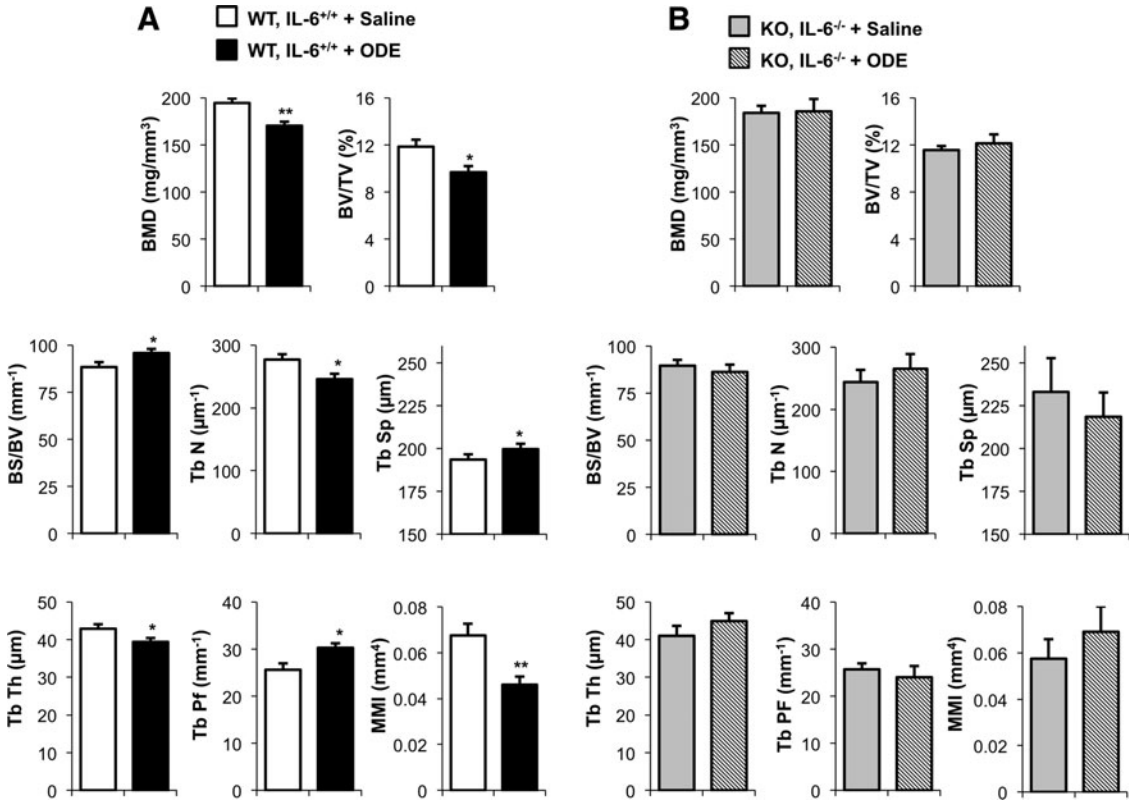

FIG. 4. Inhalant ODE exposure-induced bone quality and quantity loss is dependent on IL-6 pathway. The tibia bone of WT **(A)** and IL-6 KO **(B)** mice repetitively treated with inhalation of saline or ODE were subjected to micro-CT analysis. ODE induced significant changes in parameters of bone quality and bone quantity in WT animals, which was not demonstrated in IL-6 KO mice. Parameters include BMD, specific bone surface area (BS/BV), percent bone volume (BV/TV), specific bone surface area (BS/BV), TbN, TbSp, TbTh, TbPf, and polar MMI. Bar graphs are means with standard error bars. For WT, $n=8$ mice/group from 2 independent experiments. For IL-6 KO, $n=11$ mice/group from 3 independent experiments. Statistical significance denoted as $^{*}P<0.05$, $^{**}P<0.01$ versus saline. BMD, bone mineral density; BS/BV, bone surface to bone volume ratio; BV/TV, bone volume to tissue volume ratio; MMI, moment of inertia; TbPf, trabecular pattern factor; TbN, trabecular number; TbSp, trabecular separation; TbTh, trabecular thickness.

Expansion of bone marrow osteoclast progenitor cells accompanying inhalant ODE exposure is dependent upon IL-6

In these studies we sought to determine whether systemic IL-6 impacted OCP populations in response to repetitive inhalant ODE exposures. In the WT animals, inhalant ODE treatment resulted in increased numbers of OCPs recognized as TN $CD115^{+}CD117^{+}$ cells ($P<0.05$) and TN $CD115^{+}CD117^{+}CD27^{+}$ cells ($P<0.01$) compared to saline-treated WT mice (Fig. 6A). In contrast, there was no significant increase in OCPs in the ODE-exposed mice compared to saline control in IL-6 KO animals (Fig. 6B).

Discussion

We report several new findings regarding the role of IL-6 in the airway and systemic bone response to inhalant ODE exposures. Namely, this study finds a role for the IL-6 effector response in mediating the adverse bone consequences induced by inhaled organic dust exposures, yet lack of IL-6 did not reduce the airway inflammatory response to ODE. ODE-induced airway neutrophil influx, cytokine/chemokine release, and lung pathology remained elevated in IL-6 KO animals. Moreover, findings support a potential compensatory increase in airway inflammatory cytokines/chemokines in the absence of IL-6. In contrast, IL-6 KO animals were protected against repetitive inhalant ODE-induced bone deterioration, which was also associated with a blunted ODE-induced osteoclast progenitor response. Collectively, these studies highlight an important function for IL-6 in explaining how airway injury might be linked to bone loss manifestations.

A role for the IL-6 signaling pathway in regulating bone loss and bone deterioration has been well described in autoimmune diseases, particularly RA (Schett 2008; Karsdal and others 2012; Tanaka and others 2014; Briot and others 2015). Specifically, IL-6 signaling events induce osteoclast differentiation, which is implicated in causing joint destruction and osteoporosis associated with RA (Schett 2008; Karsdal and others 2012). IL-6 levels in serum and synovial fluid in RA patients correlate with disease activity and severity (Garnero and others 2010), and blocking the IL-6 receptor has been used successfully in the treatment of RA-induced bone disease (Karsdal and others 2012; Fleischmann and others 2013). Interestingly, others have shown a relationship with IL-6 and bone loss among nonarthritis-related diseases as elevated IL-6-induced inflammation has been shown to be responsible for obesity-associated bone loss in mice (Halade and others 2011). Our findings support an important role for

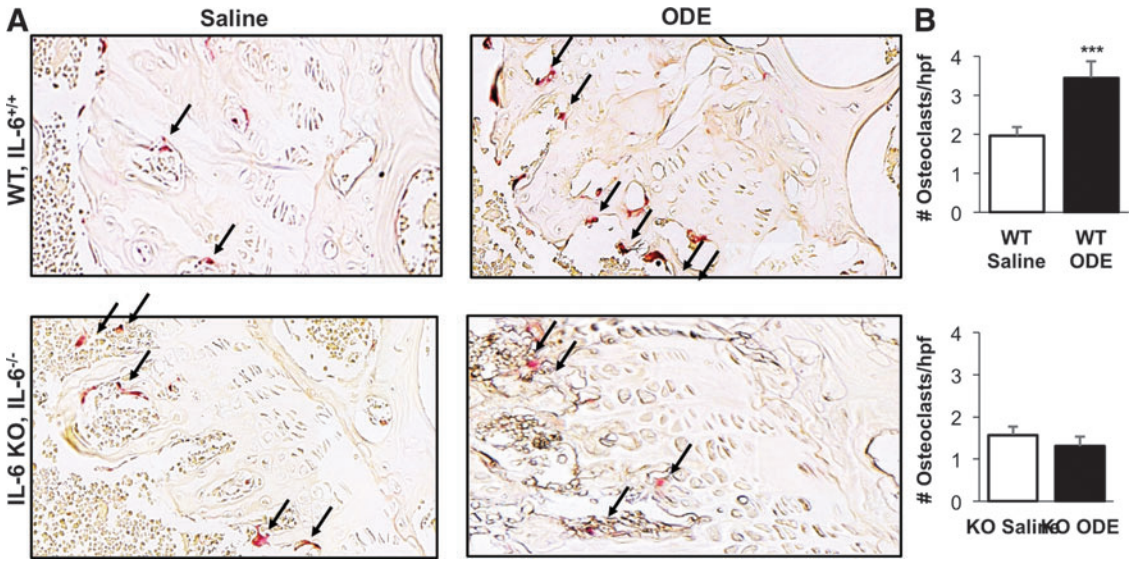

FIG. 5. Repetitive inhalational ODE exposures induce bone-resorbing osteoclasts, which is not demonstrated in IL-6 KO mice. Tibias from inhalant saline and ODE-treated animals were decalcified and multinucleated osteoclasts were identified by TRAP, which gives the characteristic magenta color. **(A)** Representative bone sections of 1 mouse per treatment group are shown at 40×. Osteoclasts (*arrows*) were more prominent in ODE-treated WT mice. **(B)** Bar graph depicts mean with standard error bars of $TRAP^+$ osteoclasts per high power field among WT and IL-6 KO treatment groups (10 microscopic fields of visions/bone and 7 bones/treatment group from a minimum of 2 independent experiments). Statistical significance denoted as $***P<0.001$ versus saline. TRAP, tartrate-resistant acid phosphatase.

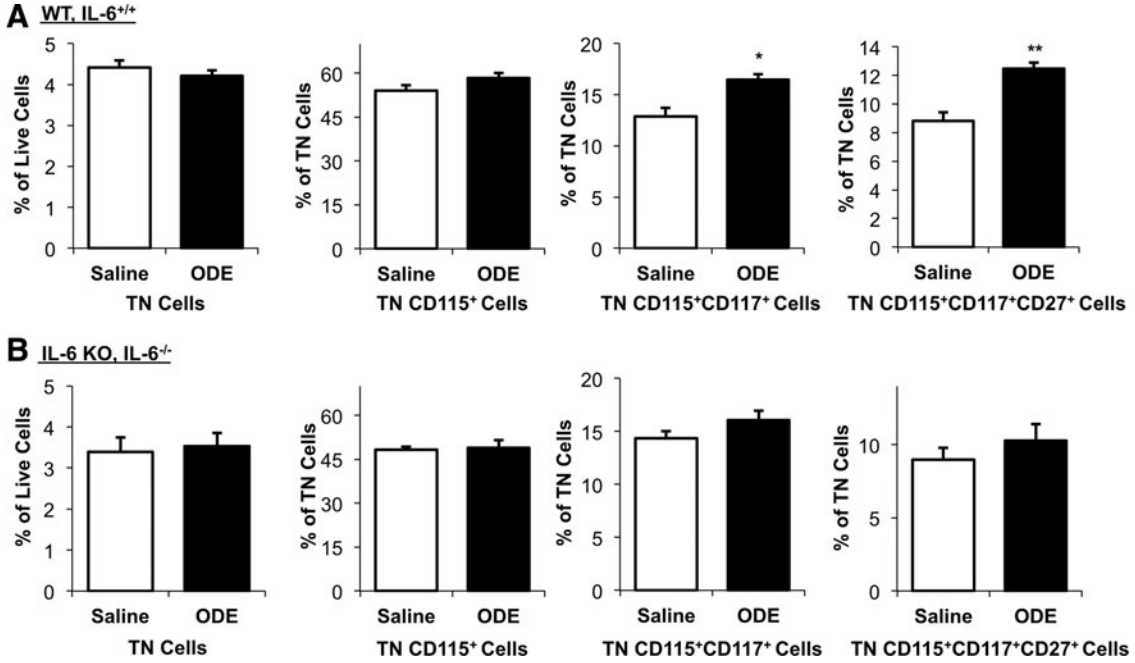

FIG. 6. Repetitive inhalational ODE exposures induce OCPs, which is not demonstrated in IL-6 KO mice. Bone marrow cells from **(A)** WT and **(B)** IL-6 KO animals treated with inhalant saline or ODE daily for 3 weeks were analyzed by flow cytometry for osteoclast progenitors. After exclusion of debris and dead cells, TN cells were gated based upon $CD45R^-CD3^-CD11b^{lo}$ phenotype. Distribution of TN cells is shown as mean percentage with SEM bars of live cells. Distribution of TN cells expressing CD115, CD115 CD117, and CD115 CD117 CD27 are shown as percentage with SEM bars of TN cells. Bone marrow cells enriched for osteoclast progenitors are noted as TN $CD115^+CD117^+$ and TN $CD115^+CD117^+CD27^+$. WT mice treated with ODE demonstrated statistically significant increase in OCP cells compared to control ($*P<0.05$ and $**P<0.01$). In contrast, there was no significant increase in OCP populations with ODE treatment in IL-6 KO mice. $n=4$ mice/group from 2 independent experiments. OCP, osteoclast precursor.

systemic IL-6 in mediating bone deterioration secondary to airway inflammation induced by complex, microbial product-enriched organic dust exposures.

Bone homeostasis is maintained through crosstalk and activities of osteoblasts (bone-forming cells) and osteoclasts (bone-resorbing cells). Osteoclasts are myeloid-derived cells, and we found increased osteoclasts in ODE-treated WT mice (Fig. 5). Furthermore, we demonstrated by flow cytometry that OCP populations (Fig. 6; TN $CD115^+CD117^+CD27^+$) are increased in bone marrow cells collected from ODE-treated WT animals. These findings were not seen in ODE-treated IL-6 KO mice. Thus, it is possible that an expansion of osteoclast progenitor cells through an IL-6-mediated pathway might represent a potential mechanism to explain inhalant ODE-induced bone loss. Collectively, these findings corroborate the micro-CT ODE-induced bone deterioration findings.

Our findings are consistent with several studies showing that IL-6 induces the differentiation of OCP cells into mature and active osteoclasts both *in vitro* and *in vivo* (Binkley and others 1994; Wong and others 2006), whereas there are other studies demonstrating an inhibitory role for IL-6 in osteoclast formation (Duplomb and others 2008; Yoshitake and others 2008; Darowish and others 2009). Specifically, Darowish and others (2009) demonstrated an anti-osteoclastogenic IL-6 effect in a murine calvarial model of titanium particle-induced osteolysis, an entirely different model system than investigated here. It is possible that this apparent contradictory role for IL-6 in the literature might be explained by the nature and setting of the inflammatory insult. In addition, positive and negative roles for the IL-6 signaling pathway in regulating osteoblastogenesis have been demonstrated (Franchimont and others 2005; Peruzzi and others 2012; Kaneshiro and others 2014). To date, we have not been able to define a role for inhalant ODE treatments affecting osteoblasts (data not shown), but recognize that future studies might be warranted.

Because of the high prevalence of both lung and musculoskeletal disease (including fractures) in agriculture workers (Leon and others 2011; Osborne and others 2012), we previously sought and demonstrated a lung inflammatory-bone loss connection in an animal model (Dusad and others 2013). Our findings of a role for IL-6 in linking lung to bone loss following agriculture dust exposures might be relevant in other air pollutants such as cigarette smoke, which is a recognized risk factor for osteoporosis leading to fracture (Yan and others 2011). In addition, our data would support determinations of serum IL-6 levels in future human lung disease-bone loss studies to determine the extent and importance of this relationship. It remains unclear as to the exact source of IL-6 responsible for mediating bone consequences, whereas it has been demonstrated that IL-6 production is dependent upon both airway epithelial cells and hematopoietic-derived cells (particularly macrophages) (Poole and others 2012b, 2015b). Other potential sources of systemic IL-6 could include liver or circulating hematopoietic cells, which could be investigated in future studies.

Increased serum IL-6 levels have been reported in asthmatic patients (Yokoyama and others 1995), and increased levels of serum IL-6 have also been shown to be predictive of increased mortality in COPD patients (Agusti and others 2012; Celli and others 2012). For these reasons, we had postulated that IL-6 KO mice would have reduced airway inflammatory manifestations compared to WT animals. However, there was no evidence of reduction in lung inflammatory disease process induced by repetitive ODE exposures, and in fact, there was evidence of increased ODE-induced cytokine/chemokine production and trends toward increased neutrophil influx in IL-6 KO mice.

These latter findings are consistent with earlier work by others demonstrating that absence of IL-6 results in an increased acute inflammatory response in endotoxic lung or endotoxemia animal models (Xing and others 1998). Namely, it was previously revealed that endogenous IL-6 plays a crucial anti-inflammatory role in regulating the local lung acute inflammatory response by controlling the level of proinflammatory cytokines (Xing and others 1998). It is also possible that other systemic cytokine effector responses are involved in mediating ODE-induced bone deterioration. However, repetitive inhalant treatments with ODE have not impacted other cytokines (ie, TNF-α, IL-1β, or IL-17 levels) that have been implicated in promoting osteoclastogenesis (Bar-Shavit 2008) and data not shown.

Our findings found here lay the foundation for future studies. It remains unknown whether IL-6 classical or IL-6 *trans* signaling pathways are driving the lung-bone IL-6-mediated response to inhalant ODE exposures. In the IL-6 classical signaling pathway, IL-6 binds to membrane IL-6Rα and associates with 2 molecules of gp130 to initiate intracellular signaling (Scheller and others 2011, 2014). In IL-6 *trans* signaling, IL-6 cytokine complexes with the soluble form of IL-6Rα associate with gp130 to initiate signaling (Scheller and others 2011, 2014). IL-6 *trans* signaling has been implicated in mediating other diseases such as asthma (Finotto and others 2007), pulmonary fibrosis (Le and others 2014), and RA (Cronstein 2007). To our knowledge, the role of shed or soluble IL-6Rα and/or IL-6 *trans* signaling in agriculture organic dust-induced lung diseases has not been investigated but would warrant future studies.

It is also possible that classical signaling pathway could be important in B cell-mediated antibody responses and influencing the acute inflammatory response to ODE exposures. Although there was no difference in lung pathology between ODE-treated WT and IL-6 KO animals, it also remains possible that the phenotype of infiltrating lymphocytes are impacted by IL-6 signaling pathway. Our prior work demonstrated that repetitive ODE exposures induce a $CD4^+$ T cells with a Th1/Th17 lung microenvironment (Poole and others 2012a) and an increase in activated $CD11c^+CD11b+$ macrophages (Poole and others 2012b). Finally, the impact of repetitive ODE treatments on muscle structure and functional physical performance is not known, but might also represent an interesting new direction of studies.

In conclusion, the systemic IL-6 effector pathway is an important component in understanding the lung-bone inflammatory axis to explain bone deterioration in the setting of repetitive exposures to inhalant ODE in a murine model. This was further corroborated with a role for IL-6 in regulating osteoclast progenitor cells and bone osteoclasts induced by inhalant exposures. These findings might also have implications for other chronic inflammatory lung diseases, such as COPD or asthma, whereby systemic IL-6 has been implicated in mediating extra-pulmonary manifestations. The availability of anti-IL-6 therapeutic approaches for

prevention of bone complications in patients with systemic inflammatory diseases also lends itself to an attractive therapy for bone complications associated with chronic airway inflammatory diseases.

Acknowledgments

The authors wish to thank the Tissue Sciences Facility at the Department of Pathology and Microbiology (University of Nebraska Medical Center, Omaha, NE) for assistance with images. This study was supported by grants from the National Institute of Environmental Health Sciences (R01: ES019325 to J.A.P.) and the National Institute of Occupational Safety Health (U54OH010162 to T.A.W. and J.A.P. and R01OH008539 to D.J.R.). This work was supported in part by the Central States Center for Agricultural Safety and Health (CS-CASH).

Author Disclosure Statement

No competing financial interests exist.

References

Agusti A, Edwards LD, Rennard SI, MacNee W, Tal-Singer R, Miller BE, Vestbo J, Lomas DA, Calverley PM, Wouters E, et al. 2012. Persistent systemic inflammation is associated with poor clinical outcomes in COPD: a novel phenotype. PLoS One 7(5):e37483.

Bar-Shavit Z. 2008. Taking a toll on the bones: regulation of bone metabolism by innate immune regulators. Autoimmunity 41(3):195–203.

Bellido M, Lugo L, Roman-Blas JA, Castaneda S, Caeiro JR, Dapia S, Calvo E, Largo R, Herrero-Beaumont G. 2010. Subchondral bone microstructural damage by increased remodelling aggravates experimental osteoarthritis preceded by osteoporosis. Arthritis Res Ther 12(4):R152.

Binkley NC, Sun WH, Checovich MM, Roecker EB, Kimmel DB, Ershler WB. 1994. Effects of recombinant human interleukin-6 administration on bone in rhesus monkeys. Lymphokine Cytokine Res 13(4):221–226.

Boissy RJ, Romberger DJ, Roughead WA, Weissenburger-Moser L, Poole JA, Levan TD. 2014. Shotgun pyrosequencing metagenomic analyses of dusts from swine confinement and grain facilities. PLoS One 9(4):e95578.

Briot K, Rouanet S, Schaeverbeke T, Etchepare F, Gaudin P, Perdriger A, Vray M, Steinberg G, Roux C. 2015. The effect of tocilizumab on bone mineral density, serum levels of dickkopf-1 and bone remodeling markers in patients with rheumatoid arthritis. Joint Bone Spine 82(2):109–115.

Celli BR, Locantore N, Yates J, Tal-Singer R, Miller BE, Bakke P, Calverley P, Coxson H, Crim C, Edwards LD, et al. 2012. Inflammatory biomarkers improve clinical prediction of mortality in chronic obstructive pulmonary disease. Am J Respir Crit Care Med 185(10):1065–1072.

Cronstein BN. 2007. Interleukin-6—a key mediator of systemic and local symptoms in rheumatoid arthritis. Bull NYU Hosp Jt Dis 65 Suppl 1:S11–S15.

Darowish M, Rahman R, Li P, Bukata SV, Gelinas J, Huang W, Flick LM, Schwarz EM, O'Keefe RJ. 2009. Reduction of particle-induced osteolysis by interleukin-6 involves anti-inflammatory effect and inhibition of early osteoclast precursor differentiation. Bone 45(4):661–668.

Dempster DW, Compston JE, Drezner MK, Glorieux FH, Kanis JA, Malluche H, Meunier PJ, Ott SM, Recker RR, Parfitt AM. 2013. Standardized nomenclature, symbols, and units for bone histomorphometry: a 2012 update of the report of the ASBMR histomorphometry nomenclature committee. J Bone Miner Res 28(1):2–17.

Duplomb L, Baud'huin M, Charrier C, Berreur M, Trichet V, Blanchard F, Heymann D. 2008. Interleukin-6 inhibits receptor activator of nuclear factor kappaB ligand-induced osteoclastogenesis by diverting cells into the macrophage lineage: key role of Serine727 phosphorylation of signal transducer and activator of transcription 3. Endocrinology 149(7):3688–3697.

Dusad A, Thiele GM, Klassen LW, Gleason AM, Bauer C, Mikuls TR, Duryee MJ, West WW, Romberger DJ, Poole JA. 2013. Organic dust, lipopolysaccharide, and peptidoglycan inhalant exposures result in bone loss/disease. Am J Respir Cell Mol Biol 49(5):829–836.

Dusad A, Thiele GM, Klassen LW, Wang D, Duryee MJ, Mikuls TR, Staab EB, Wyatt TA, West WW, Reynolds SJ, et al. 2015. Vitamin D supplementation protects against bone loss following inhalant organic dust and lipopolysaccharide exposures in mice. Immunol Res 62(1):46–59.

Ek A, Palmberg L, Larsson K. 2004. The effect of fluticasone on the airway inflammatory response to organic dust. Eur Respir J 24(4):587–593.

Ferrari R, Tanni SE, Caram LM, Correa C, Correa CR, Godoy I. 2013. Three-year follow-up of interleukin 6 and C-reactive protein in chronic obstructive pulmonary disease. Respir Res 14:24.

Finotto S, Eigenbrod T, Karwot R, Boross I, Doganci A, Ito H, Nishimoto N, Yoshizaki K, Kishimoto T, Rose-John S, et al. 2007. Local blockade of IL-6R signaling induces lung CD4+ T cell apoptosis in a murine model of asthma via regulatory T cells. Int Immunol 19(6):685–693.

Fleischmann RM, Halland AM, Brzosko M, Burgos-Vargas R, Mela C, Vernon E, Kremer JM. 2013. Tocilizumab inhibits structural joint damage and improves physical function in patients with rheumatoid arthritis and inadequate responses to methotrexate: LITHE study 2-year results. J Rheumatol 40(2): 113–126.

Franchimont N, Wertz S, Malaise M. 2005. Interleukin-6: an osteotropic factor influencing bone formation? Bone 37(5): 601–606.

Garnero P, Thompson E, Woodworth T, Smolen JS. 2010. Rapid and sustained improvement in bone and cartilage turnover markers with the anti-interleukin-6 receptor inhibitor tocilizumab plus methotrexate in rheumatoid arthritis patients with an inadequate response to methotrexate: results from a substudy of the multicenter double-blind, placebo-controlled trial of tocilizumab in inadequate responders to methotrexate alone. Arthritis Rheum 62(1):33–43.

Graat-Verboom L, Smeenk FW, van den Borne BE, Spruit MA, Donkers-van Rossum AB, Aarts RP, Wouters EF. 2012. Risk factors for osteoporosis in caucasian patients with moderate chronic obstructive pulmonary disease: a case control study. Bone 50(6):1234–1239.

Hahn M, Vogel M, Pompesius-Kempa M, Delling G. 1992. Trabecular bone pattern factor—a new parameter for simple quantification of bone microarchitecture. Bone 13(4): 327–330.

Halade GV, El Jamali A, Williams PJ, Fajardo RJ, Fernandes G. 2011. Obesity-mediated inflammatory microenvironment stimulates osteoclastogenesis and bone loss in mice. Exp Gerontol 46(1):43–52.

Jacome-Galarza C, Soung DY, Adapala NS, Pickarski M, Sanjay A, Duong LT, Lorenzo J, Drissi H. 2014. Altered

hematopoietic stem cell and osteoclast precursor frequency in cathepsin K null mice. J Cell Biochem 115(8):1449–1457.
Jung JW, Kang HR, Kim JY, Lee SH, Kim SS, Cho SH. 2014. Are asthmatic patients prone to bone loss? Ann Allergy Asthma Immunol 112(5):426–431.
Kaneshiro S, Ebina K, Shi K, Higuchi C, Hirao M, Okamoto M, Koizumi K, Morimoto T, Yoshikawa H, Hashimoto J. 2014. IL-6 negatively regulates osteoblast differentiation through the SHP2/MEK2 and SHP2/Akt2 pathways in vitro. J Bone Miner Metab 32(4):378–392.
Karsdal MA, Schett G, Emery P, Harari O, Byrjalsen I, Kenwright A, Bay-Jensen AC, Platt A. 2012. IL-6 receptor inhibition positively modulates bone balance in rheumatoid arthritis patients with an inadequate response to anti-tumor necrosis factor therapy: biochemical marker analysis of bone metabolism in the tocilizumab RADIATE study (NCT00106522). Semin Arthritis Rheum 42(2):131–139.
Krisher T, Bar-Shavit Z. 2014. Regulation of osteoclastogenesis by integrated signals from toll-like receptors. J Cell Biochem 115(12):2146–2154.
Lahousse L, van den Bouwhuijsen QJ, Loth DW, Joos GF, Hofman A, Witteman JC, van der Lugt A, Brusselle GG, Stricker BH. 2013. Chronic obstructive pulmonary disease and lipid core carotid artery plaques in the elderly: the rotterdam study. Am J Respir Crit Care Med 187(1):58–64.
Le TT, Karmouty-Quintana H, Melicoff E, Le TT, Weng T, Chen NY, Pedroza M, Zhou Y, Davies J, Philip K, et al. 2014. Blockade of IL-6 trans signaling attenuates pulmonary fibrosis. J Immunol 193(7):3755–3768.
Lehouck A, Boonen S, Decramer M, Janssens W. 2011. COPD, bone metabolism, and osteoporosis. Chest 139(3):648–657.
Leon ME, Beane Freeman LE, Douwes J, Hoppin JA, Kromhout H, Lebailly P, Nordby KC, Schenker M, Schuz J, Waring SC, et al. 2011. AGRICOH: a consortium of agricultural cohorts. Int J Environ Res Public Health 8(5):1341–1357.
May S, Romberger DJ, Poole JA. 2012. Respiratory health effects of large animal farming environments. J Toxicol Environ Health B Crit Rev 15(8):524–541.
Monso E, Schenker M, Radon K, Riu E, Magarolas R, McCurdy S, Danuser B, Iversen M, Saiki C, Nowak D. 2003. Region-related risk factors for respiratory symptoms in European and Californian farmers. Eur Respir J 21(2):323–331.
Osborne A, Blake C, Fullen BM, Meredith D, Phelan J, McNamara J, Cunningham C. 2012. Prevalence of musculoskeletal disorders among farmers: a systematic review. Am J Ind Med 55(2):143–158.
Pauwels NS, Bracke KR, Maes T, Pilette C, Joos GF, Brusselle GG. 2010. The role of interleukin-6 in pulmonary and systemic manifestations in a murine model of chronic obstructive pulmonary disease. Exp Lung Res 36(8):469–483.
Peruzzi B, Cappariello A, Del Fattore A, Rucci N, De Benedetti F, Teti A. 2012. c-src and IL-6 inhibit osteoblast differentiation and integrate IGFBP5 signalling. Nat Commun 3:630.
Poole JA, Dooley GP, Saito R, Burrell AM, Bailey KL, Romberger DJ, Mehaffy J, Reynolds SJ. 2010. Muramic acid, endotoxin, 3-hydroxy fatty acids, and ergosterol content explain monocyte and epithelial cell inflammatory responses to agricultural dusts. J Toxicol Environ Health A 73(10):684–700.
Poole JA, Gleason AM, Bauer C, West WW, Alexis N, Reynolds SJ, Romberger DJ, Kielian T. 2012a. Alphabeta T cells and a mixed Th1/Th17 response are important in organic dust-induced airway disease. Ann Allergy Asthma Immunol 109(4):266,273.e2.
Poole JA, Gleason AM, Bauer C, West WW, Alexis N, van Rooijen N, Reynolds SJ, Romberger DJ, Kielian TL. 2012b. CD11c+/CD11b+ cells are critical for organic dust-elicited murine lung inflammation. Am J Respir Cell Mol Biol 47(5):652–659.
Poole JA, Romberger DJ, Wyatt TA, Staab E, VanDeGraaff J, Thiele GM, Dusad A, Klassen LW, Duryee MJ, Mikuls TR, et al. 2015a. Age impacts pulmonary inflammation and systemic bone response to inhaled organic dust exposure. J Toxicol Environ Health A 78(19):1201–1216.
Poole JA, Wyatt TA, Oldenburg PJ, Elliott MK, West WW, Sisson JH, Von Essen SG, Romberger DJ. 2009. Intranasal organic dust exposure-induced airway adaptation response marked by persistent lung inflammation and pathology in mice. Am J Physiol Lung Cell Mol Physiol 296(6):L1085–L1095.
Poole JA, Wyatt TA, Romberger DJ, Staab E, Simet S, Reynolds SJ, Sisson JH, Kielian T. 2015b. MyD88 in lung resident cells governs airway inflammatory and pulmonary function responses to organic dust treatment. Respir Res 16(1):111.
Scheller J, Chalaris A, Schmidt-Arras D, Rose-John S. 2011. The pro- and anti-inflammatory properties of the cytokine interleukin-6. Biochim Biophys Acta 1813(5):878–888.
Scheller J, Garbers C, Rose-John S. 2014. Interleukin-6: from basic biology to selective blockade of pro-inflammatory activities. Semin Immunol 26(1):2–12.
Schett G. 2008. Review: immune cells and mediators of inflammatory arthritis. Autoimmunity 41(3):224–229.
Sin DD, Macnee W. 2013. Chronic obstructive pulmonary disease and cardiovascular diseases: a ''vulnerable'' relationship. Am J Respir Crit Care Med 187(1):2–4.
Tanaka T, Narazaki M, Ogata A, Kishimoto T. 2014. A new era for the treatment of inflammatory autoimmune diseases by interleukin-6 blockade strategy. Semin Immunol 26(1):88–96.
Thiolat A, Semerano L, Pers YM, Biton J, Lemeiter D, Portales P, Quentin J, Jorgensen C, Decker P, Boissier MC, et al. 2014. Interleukin-6 receptor blockade enhances CD39+ regulatory T cell development in rheumatoid arthritis and in experimental arthritis. Arthritis Rheumatol 66(2):273–283.
Wang Z, Larsson K, Palmberg L, Malmberg P, Larsson P, Larsson L. 1997. Inhalation of swine dust induces cytokine release in the upper and lower airways. Eur Respir J 10(2):381–387.
Wang Z, Malmberg P, Larsson P, Larsson BM, Larsson K. 1996. Time course of interleukin-6 and tumor necrosis factor-alpha increase in serum following inhalation of swine dust. Am J Respir Crit Care Med 153(1):147–152.
Wong PK, Quinn JM, Sims NA, van Nieuwenhuijze A, Campbell IK, Wicks IP. 2006. Interleukin-6 modulates production of T lymphocyte-derived cytokines in antigen-induced arthritis and drives inflammation-induced osteoclastogenesis. Arthritis Rheum 54(1):158–168.
Xiao Y, Song JY, de Vries TJ, Fatmawati C, Parreira DB, Langenbach GE, Babala N, Nolte MA, Everts V, Borst J. 2013. Osteoclast precursors in murine bone marrow express CD27 and are impeded in osteoclast development by CD70 on activated immune cells. Proc Natl Acad Sci U S A 110(30):12385–12390.
Xing Z, Gauldie J, Cox G, Baumann H, Jordana M, Lei XF, Achong MK. 1998. IL-6 is an antiinflammatory cytokine required for controlling local or systemic acute inflammatory responses. J Clin Invest 101(2):311–320.

Yan C, Avadhani NG, Iqbal J. 2011. The effects of smoke carcinogens on bone. Curr Osteoporos Rep 9(4):202–209.

Yokoyama A, Kohno N, Fujino S, Hamada H, Inoue Y, Fujioka S, Ishida S, Hiwada K. 1995. Circulating interleukin-6 levels in patients with bronchial asthma. Am J Respir Crit Care Med 151(5):1354–1358.

Yoshida Y, Tanaka T. 2014. Interleukin 6 and rheumatoid arthritis. Biomed Res Int 2014:698313.

Yoshitake F, Itoh S, Narita H, Ishihara K, Ebisu S. 2008. Interleukin-6 directly inhibits osteoclast differentiation by suppressing receptor activator of NF-kappaB signaling pathways. J Biol Chem 283(17):11535–11540.

Zhiping W, Malmberg P, Larsson BM, Larsson K, Larsson L, Saraf A. 1996. Exposure to bacteria in swine-house dust and acute inflammatory reactions in humans. Am J Respir Crit Care Med 154(5):1261–1266.

Address correspondence to:
Dr. Jill A. Poole
Pulmonary, Critical Care, Sleep & Allergy Division
Department of Medicine
University of Nebraska Medical Center
The Nebraska Medical Center
Omaha, NE 68198 5990

E-mail: lchudome@unmc.edu

Received 16 May 2016/Accepted 12 August 2016